Monomer-dimer random laser model

P. Vaveliuk, A. M. de Brito Silva, and P. C. de Oliveira
Departamento de Física, Universidade Federal da Paraíba,
Caixa Postal 5008, João Pessoa, Paraíba 58051-970, Brazil

In this work we present a model for the bichromatic laser emission from laser dye solutions containing randomly distributed scattering particles. We suggest that the bichromatic emission is produced by two fluorescent aggregates: monomers and dimers. The shorter-wavelength laser peak was attributed to the monomer emission and the secondary longer-wavelength peak was attributed to the dimer emission. From neat dye solutions, using absorption and emission spectroscopies, the monomer and dimer absorption and emission cross sections were obtained. The partial overlap between the dimer absorption cross section and the monomer emission cross section indicates an unidirectional radiative and nonradiative energy transfer from excited monomers to fundamental dimers. The dynamics of the laser emission was modelled by a set of rate equations, which solutions agree with our experimental data. It is also showed that nonradiative energy transfer plays a very important role in the dimer laser process, and helps to explain the relatively strong dimer laser peak intensities.

I. INTRODUCTION

The observation of laserlike emission in active scattering media has been attracting the interest in the investigation of disordered dielectric microstructures as alternative sources of coherent light. This phenomenon was observed in laser dye solutions[1], dye doped solid polymer matrices [2–4], as well as laser crystal powders [5]. From a theoretical point of view, the effect was first predicted by Letokhov [6] who suggest non-resonant feedback of diffusive photons in the random scattering medium with gain. Letokhov's work was the start point to the development of several models that attempted to explain the experimental results in the different random systems.

In this paper a laser model is presented which describes the evolution of electronic excited states of monomers and dimers, and the evolution of stimulated emission in the scattering medium with gain by a set of rate equations. Our laser model is based on the enhanced and spectral narrowing of the light produced by the absorbing dye (active medium) and by the scattering with colloidal particles suspended in the solution. The laser gain threshold, γ_{th}, depends on the balance between gain and loss of light in the system. In an active scattering medium, the loss as well as the amplified path lengths, and hence the laser threshold depends on the size of the pumped volume. The feedback is supplied by the scattering particles where incomplete feedback gives rise to the loss. The spatial distribution of gain is governed by the spreading of pump light in the system. The amplification increases exponentially with the total distance traversed by the lasing photons in the gain medium. The spatial distribution geometry involves a cylindrical volume of diameter of the excitation spot and penetration length L_p, determined by photon transport mean free path l and by the absorption length l_a, which is inversely proportional to the dye absorption coefficient, through the well-known relation $L_p = (ll_a/3)^{1/2}$ [7, 8]. The laser gain threshold can be quantified by a Monte Carlo method, following the procedure employed in refs. [9, 10]. Then, γ_{th} was used in the monomer-dimer laser model in order to calculate the population inversion and the laser emitted photons. The rate equations are given in terms of fraction of monomer and dimer densities in the excited state, $n_m = N_M^1/N_M$ and $n_d = N_D^1/N_D$, and in terms of emission photon number per unit area per unit time, $\Phi_\ell[photons/(cm^2 ns)]$. For the monomer and dimer excited population evolution we have

$$\begin{aligned}
\frac{d}{dt}n_m(t) &= [1-n_m(t)]\,\sigma_M^{abs}(\lambda_P)\,\Phi_P(t) \\
&\quad -n_m(t)\,\frac{1}{\tau_M} - n_m(t)\int d\lambda \sigma_M^{em}(\lambda)\,\Phi_\ell(\lambda,t) \\
&\quad +[1-n_m(t)]\int d\lambda \sigma_M^{abs}(\lambda)\,\Phi_\ell(\lambda,t) \\
&\quad -K_{fnet}N_D n_m(t)\,[1-n_d(t)]\,, \qquad (1) \\
\frac{d}{dt}n_d(t) &= [1-n_d(t)]\,\sigma_D^{abs}(\lambda_P)\,\Phi_P(t) \\
&\quad -n_d(t)\,\frac{1}{\tau_D} - n_d(t)\int d\lambda \sigma_D^{em}(\lambda)\,\Phi_\ell(\lambda,t) \\
&\quad +[1-n_d(t)]\int d\lambda \sigma_D^{abs}(\lambda)\,\Phi_\ell(\lambda,t) \\
&\quad +K_{fnet}N_M n_m(t)\,[1-n_d(t)]\,. \qquad (2)
\end{aligned}$$

The physical picture that have been taken into account in these equations is as follows. Two active aggregates, monomers and dimers with equilibrium densities N_M and N_D compose the dye solution. The absorbing dye solution, i.e. monomers and dimers, is excited by a monochromatic pumping beam of intensity I_P at excitation wavelength λ_P. When a number of pump photons per unit area per unit time, $\Phi_P = I_P/h\nu$, is incident on the sample, it results in the simultaneous excitation of monomers and dimers from the ground state 0 to first excited state 1 as showed in Fig. 1. These processes take place at rates given by $\sigma_M^{abs}(\lambda_P)\,\Phi_P$ for monomers and $\sigma_D^{abs}(\lambda_P)\,\Phi_P$ for dimers, where σ_i^{abs} $(i = M, D)$ are the monomer and dimer absorption cross-section at the

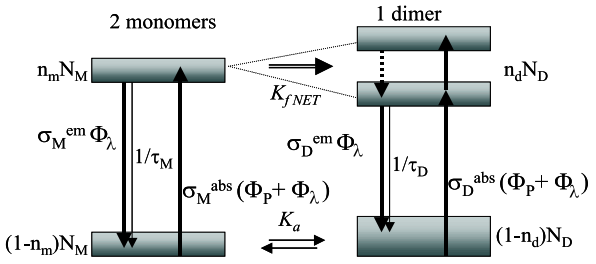

FIG. 1: Simplified scheme of fundamental and first excited energy levels of dye solution composed by monomers of total density N_M and dimers of total density N_D. n_m and n_d indicate the fraction of monomers and dimers in the excited states. The arrows indicate the principal energy transfer processes, with their respective rates, that occur when the dye molecules are excited by laser radiation of photon flux Φ_P.

pump wavelength λ_P. The first term in Eqs. 1 and 2 indicates these processes. The second term indicates the fractions of the excited monomer and dimer n_m and n_d that relax to their respective ground states via radiative (spontaneous) and nonradiative decay with a rate given by

$$\frac{1}{\tau_i} = \frac{1}{\tau_i^r} + \frac{1}{\tau_i^{nr}}, \quad i = M, D, \tag{3}$$

where $\tau_{M,D}$ is the monomer (dimer) excited state lifetime (symbolized by the thin arrow in the Fig. 1). $\tau_{M,D}^r$ symbolize the monomer (dimer) radiative lifetime that can be directly calculated from the absorption and fluorescence spectra from the well-known Strickler-Berg relation [11, 12]

$$\frac{1}{\tau_i^r} = 7.54 \times 10^9 n_{ref}^2 \frac{\int_{fl} F_i(\lambda)\, \lambda d\lambda}{\int_{fl} F_i(\lambda)\, \lambda^4 d\lambda} \int_{abs} \sigma_i^{abs}(\lambda)\, \lambda^{-1} d\lambda, \tag{4}$$

where the integration is performed over the fluorescence and absorption bands and n_{ref} is the average refractive index. $\tau_{M,D}^{nr}$ symbolize the monomer (dimer) nonradiative lifetime, responsible to quenches the laser action and increases the laser threshold. For monomers, it is licit neglect the internal conversion process since for rhodamine dyes in low viscosity solvent as methanol and at room temperature, the radiative decay process from first excited state to fundamental one is very efficient close to unit [12–14]. On the contrary, the nonradiative process for dimers would be important because the simultaneous presence in the solution of fluorescent as well as non fluorescent dimers. This combination produces that the radiative dimer quantum efficiency is ranged in a wide interval values depending on the population of each dimer species in equilibrium. In weakly polar solvents as methanol, used by us in the experiments, the formation of fluorescent dimers is more efficient weakening the nonradiative process. Radiative as well as nonradiative process will be considered in our calculation. From Eq. 4, the value for τ_M^r was 8.3 ns. In the numerical calculus, we assume a monomer radiative quantum efficiency $\phi_M^r = 0.95$, such as the excited state lifetime $\tau_M = \tau_M^r \phi_M^r$ was 8 ns. On the other hand, the dimer excited state lifetime adopted in our calculations was also $\tau_D = 8$ ns. The calculated radiative decay lifetime from Eq. 4 was $\tau_M^r = 14.2$ ns. Therefore, these values suggest a value of the dimer radiative quantum efficiency ϕ_D^r in methanol solutions of $\phi_D^r = \tau_D^r/\tau_D = 0.56$, such as the internal conversion process is important and about half of excited molecules decays in nonradiative form.

The third term, symbolized by the thick arrow in Fig. 1, represents the decay of both manifolds from the excited state 1 to fundamental state 0 by the stimulated emission process, which occurs at rate $\sigma_M^{em}(\lambda)\Phi_\ell(\lambda)$ for monomers and $\sigma_D^{em}(\lambda)\Phi_\ell(\lambda)$ for dimers, where σ_i^{em} $(i = M, D)$ are the monomer and dimer emission cross section at the wavelength λ, and $\Phi_\ell(\lambda)$ is the number of emitted quanta at the wavelength λ. The contribution for all the wavelengths are taken into account by the integral. The fourth term represents the absorption of the dye emitted radiation $\Phi_\ell(\lambda)$ from reabsorption or radiative energy transfer process. The rate of these processes are $\sigma_M^{abs}(\lambda)\Phi_\ell(\lambda)$ for absorber monomers and $\sigma_D^{em}(\lambda)\Phi_\ell(\lambda)$ for absorber dimers at the wavelength λ. The integral takes into account the contribution over all the wavelengths. Finally, the last term represents the nonradiative energy transfer mechanism between both aggregates. Only the forward NET is taken into account in the rate equations. This is due to the strong overlap of $\sigma_M^{em}(\lambda)$ and $\sigma_D^{abs}(\lambda)$ and the practically null overlap between $\sigma_D^{em}(\lambda)$ and $\sigma_M^{abs}(\lambda)$ derived in our experiments, which makes that the nonradiative energy to be transferred in the unidirectional process $M^* + D \rightharpoonup M + D^*$. Then, this process depends on the excited state monomer population density, fundamental state dimer population density and the transfer rate K_{fNET}. Now, we shall analyze the rate equation for photon production

$$\frac{d}{dt}\Phi_\ell(\lambda, t) = \frac{c}{n}\left[\alpha(\lambda, t) - \gamma_{th}\right]\Phi_\ell(\lambda, t) + W_{sp}(\lambda, t). \tag{5}$$

The first term represents the net gain experienced by the photon in the gain medium, where c is the vacuum light speed, n is the solution refraction index, $\alpha(\lambda, t)$ is the gain coefficient at a wavelength λ which contain monomer as well as dimer contributions.

$$\alpha(\lambda, t) = \alpha_M(\lambda, t) + \alpha_D(\lambda, t), \tag{6}$$

with the gain coefficients of monomers and dimers given by

$$\alpha_M(\lambda, t) = \left\{\sigma_M^{em}(\lambda)\, n_m(t) - \sigma_M^{abs}(\lambda)\left[1 - n_m(t)\right]\right\} N_M, \tag{7}$$

$$\alpha_D(\lambda, t) = \left\{\sigma_D^{em}(\lambda)\, n_d(t) - \sigma_D^{abs}(\lambda)\left[1 - n_d(t)\right]\right\} N_D, \tag{8}$$

and γ_{th} is the threshold gain obtained by a Monte Carlo simulation method, following the procedure employed in

refs. [9, 10], given by $\gamma_{th} = 47\ cm^{-1}$ for the scatterer density employed in our experiments: $10\ mg/cm^3$. The magnitude $W_{sp}(\lambda, t)$ is the rate of spontaneous emission responsible for the initiation of laser action that contain both species spontaneous contribution. This term depends on both emission cross section, lifetime of excited species, population of excited states and is given by

$$W_{sp}(\lambda, t) = \frac{\xi_M}{\tau_M^r}\sigma_M^{em}(\lambda)\, n_m(t) + \frac{\xi_D}{\tau_D^r}\sigma_D^{em}(\lambda)\, n_d(t), \quad (9)$$

where $\xi_{M,D}$ are geometrical and spectral factors that determine the fraction of spontaneously emitted photons that goes into the build-up of the laser emission.

To solve the differential equations 1-2 and 5, we discretize Eqs. 1-2 in λ by replacing the integrals by sums. Then, Eq. 5 becomes a set of equations for each discrete λ-value that contemplates Φ_ℓ over all λ absorption plus emission region. Then, this system was numerically solved employing a fifth-order Runge-Kutta method. The resulting laser photon density $\Phi_\ell(\lambda, t)$ was integrated over time to obtain the theoretical emission spectrum to be compared with the measured spectrum by the optical multichannel analyzer.

II. THE EXPERIMENTS

In the laser emission experiments, the samples was placed in a 1 mm cuvette and was optically pumped by a frequency doubled and Q-switched Nd:YAG laser. The pump laser pulse duration was 5 ns, the repetition rate was 10 Hz and was expanded as plane wave and focused into 3 mm spot In order to analyze the dimer influence, several concentrations of Rhodamine 640 ranged from 10^{-5} to 10^{-2} M with TiO_2 nanoparticles scatterers ($\simeq 250\,nm$) were combined in a methanol solution. The scatterer concentration was $10\ mg/cm^3$. This corresponds to concentrations of the order of $10^{11}\ particles/cm^3$. The energy of the pump beam was varied from 4 μJ to 26 mJ in order to study its influence into the monomer-dimer emission relation behavior. The record of the data was done by using an Ocean Optics fiber optic spectrometer with resolution of about 0.7 nm.

Our laser emission experiments from Rhodamine 640 in methanol solutions containing a colloidal suspension of titanium dioxide particles TiO_2 show two well defined narrow lineshapes and the same qualitative behavior were observed from other Rhodamine dyes (Rh 6G and Rh 610). For the laser emission analysis, this is a crucial advantage with respect to the neat dye solution, where the emission spectrum is given by non well-defined and broad lineshapes that generally hides the presence of additional components. Fig. 2 show these results. Several features can be observed in this figure. The secondary peak tends to increase with an increasing of both, the concentration and the pump energy. The increasing of concentration indicates the increasing of the dimer population and the increase of the pump energy produces

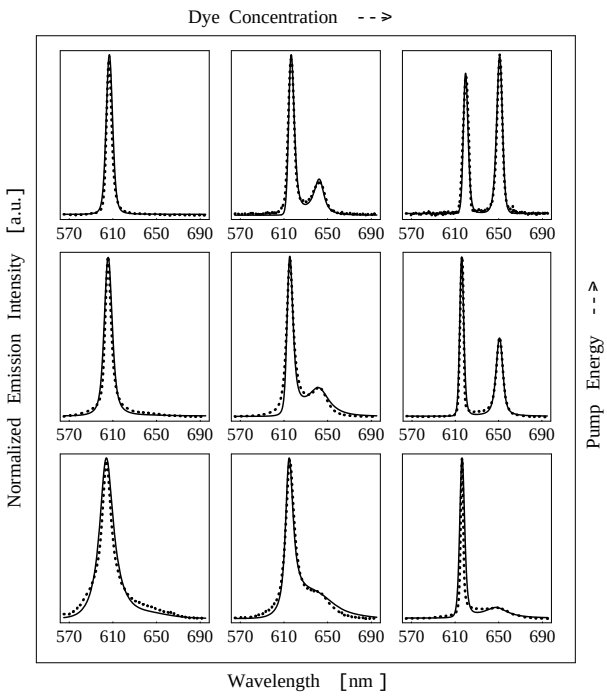

FIG. 2: Comparison between numerical solutions of the rate equations model with experimental emission spectra of Rhodamine 640 in methanol solution containing $10\ g/cm^3$ of TiO_2 scattering particles. The dashed lines represent the experimentally measured spectra and the solid lines represent the theoretical curves from the monomer-dimer laser rate equations. The rows indicate several pump energies (0.4, 2, 10 and 26 mJ, respectively, from bottom to top) and the columns indicate several dye concentrations (10^{-4}, 10^{-3}, and 10^{-2} M, respectively, from left to right).

a major radiative and nonradiative energy transfer from monomer to dimer. In particular, the reabsorption produce a slight red-shift of the emission peak when the pump energy increases. At very low intensities, no matter the dye concentration value, the spectra are broadened, as in typical fluorescence emission spectra of the neat rhodamine 640 dye. The broadening of the spectrum, when the concentration increases, indicates the dimer contribution to fluorescence. The dimer fluorescence is negligible for concentrations $\leq 10^{-4}$ M ($N_D/N_M \leq 0.028$) and both contributions are similar and strongly overlapped at $C = 10^{-2}$ M ($N_D/N_M = 1$). The laser action is not yet activated since the energy is below the threshold. The good agreement between the experimental and calculated results shows that the monomer-dimer model contemplates this feature. Now, we analyze in terms of the concentration. For $C = 10^{-4}$ M a single peak appears no matter the intensity value. Similar results were obtained for $C = 5 \times 10^{-5}$ and 10^{-5} M, which indicates that for these low concentrations only the monomer participates on the dynamics due to very low population of dimer with respect to the monomers (see Table). The activation of laser process with an increase of the pump in-

tensity [9] is evidenced by the sharpening of dye emission. For these single peak results our model coincides with that proposed by Balachandran and Lawandy [10] for a single species responsible for the emission. But, when the dye concentration increases, the dimer contribution becomes important and a second peak begins to appear, which is clearly noted in the figure at $C = 10^{-3}\ M$ ($N_D/N_M = 0.211$). The intensity of the dimer peak increases with respect to the monomer one when the pump energy increases. At high intensities, both peaks are well-defined, although the relative intensity of the dimer peak is small. At $C = 10^{-2}\ M$, the solution has the same amount of monomers and dimers in equilibrium. One can appreciate the broadening of fluorescence spectrum where both contributions are strongly overlapped for energies below the threshold. When energy increases, both contributions begin to separate and the monomer start to lase first due to $\sigma_M^{em} > \sigma_D^{em}$ making the monomer gain greater than the dimer one. When the pump energy increases even more, the dimer peak increases with respect to monomer and the laser emission is produced for both species. At high intensities, $I_p = 26\ mJ$, the dimer emission surpass the monomer one. If the energy transfer from monomers to dimers were negligible, this result would be contradictory, since the emission cross section of the dimer is smaller than the monomer one. Then, we attribute the stronger dimer emission to radiative and non-radiative energy transfer from the monomers. It is well known that the population of the excited levels of monomers increases with the pump energy, and the dimer fundamental population density increases with the concentration. Then, one could expect the rate of the forward NET, which depends on the excited monomer and fundamental dimer densities, to increase with an increasing of the dye concentration and pump energy. This was confirmed in the model simulations.

III. CONCLUSION

In this work we suggest that the bichromatic laser emission from laser dye solutions containing scattering random media is due to the presence of two fluorescent aggregates: monomers and dimers. The principal shorter-wavelength laser peak was attributed to the monomer emission and the secondary longer-wavelength peak was attributed to the dimer emission. The coexistence of monomers and dimers was confirmed from neat dye concentration in experiments of absorption and emission spectroscopies. From these experiments the monomer and dimer absorption and emission cross sections were obtained, showing a partial overlap between the dimer absorption cross section and monomer emission cross section and an absence of overlapping between the monomer absorption cross section and dimer emission cross section. This indicates an unidirectional energy transfer from excited monomer to fundamental dimers. The two molecular species contributing for the total laser emission was modelled by means of a set of rate equations for the evolution of both species excited states and the dye photon production. We have included the most important effects of energy transfer from the monomers to dimers, such as radiative energy transfer (reabsorption), but also the forward non-radiative energy transfer (fNET). The results of the monomer-dimer laser model agree very well with our experimental data.

Acknowledgments

The authors would like to thank CNPq and CTPetro-FINEP Brazilian agencies for funding this work. P.V. is a DCR-CNPq fellow and A.M.B.S. is a PIBIC-CNPq fellow.

[1] N. M. Lawandy, R. M. Balachandran, A. S. L. Gomes and E. Sauvain, *Nature (London)* **368**, 436 (1994).
[2] H. Cao, Y. G. Zhao, H. C. Ong, S. T. Ho, J. Y. Dai, J. Y. Wu and R. P. H. Chang, Appl. Phys. Lett. **73**, 3656 (1998).
[3] R. M. Balachandran, D. P. Pacheco and N. M. Lawandy, Appl. Opt. **35**, 640 (1996).
[4] S. V. Frolov, Z. V. Vardeny and K. Yoshino, Phys. Rev. B **57**, 1985 (1998).
[5] H. Cao, J. Y. Xu, S. H. Chang and S. T. Ho, Phys. Rev. E **61**, 1985 (2000).
[6] V. S. Letokhov, *Zh. Eksp. Teor. Fiz. 53, 1442 (1967)* [Sov. Phys. JETP **26**, 835 (1968)]; R. V. Ambartsumyan, N. G. Basov, P. G. Kryukov and V. S. Letokhov, *Non-Resonant Feedback in Lasers* (Pergamon Press, Oxford 1970).
[7] D. S. Wiersma and A. Lagendijk, Phys. Rev. E **54**, 4256 (1996).
[8] S. John and G. Pang, Phys. Rev. A **54**, 3642 (1996).
[9] R. M. Balachandran, N. M. Lawandy and J. A. Moon, Opt. Lett. **22**, 319 (1997).
[10] R. M. Balachandran and N. M. Lawandy, Opt. Lett. **21**, 1603 (1996).
[11] F. P. Schäfer, chap. 1: *Principles of Dye Laser Operation*, pp. 30-34 in *Dye Lasers*, edited by F. P. Schäfer (Springer-Verlag, Berlin, 1977) .
[12] A. Penzkofer and W. Leupacher, *J. Lumin.* **37**, 61 (1987).
[13] T. P. Burghardt, J. E. Lyke and K. Ajtai, *Biophys. Chem.* **59**, 119, (1996).
[14] J. Georges, *Spectrochim. Acta A* **51**, 985 (1995).